Effects of Hypoxic Preconditioning on Synaptic Ultrastructure in Mice

YI LIU,[1,2,3] ZHISHAN SUN,[1,4] SHUFENG SUN,[5] YUNXIA DUAN,[1] JINGFEI SHI,[1] ZHIFENG QI,[1] RAN MENG,[1] YONGXIN SUN,[1] XIANWEI ZENG,[4] DEHUA CHUI,[6] AND XUNMING JI[1]*

[1]*China-America Joint Institute of Neuroscience, CAJIN, Xuanwu Hospital, Capital Medical University, Beijing, China*

[2]*Neuroprotection Research Laboratory, Department of Radiology, Massachusetts General Hospital, Harvard Medical School, Boston, Massachusetts*

[3]*Neuroprotection Research Laboratory, Department of Neurology, Massachusetts General Hospital, Harvard Medical School, Boston, Massachusetts*

[4]*Department of Neurosurgery, Affiliated Hospital of Weifang Medical College, Weifang, China*

[5]*Center for Biological Electron Microscopy, Institute of Biophysics, Chinese Academy of Sciences, Beijing 100101, China*

[6]*Neuroscience Research Institute and Department of Neurobiology, Key Laboratory for Neuroscience, Ministry of Education, Ministry of Public Health, Peking University Health Science Center, Beijing 100191, China*

KEY WORDS hypoxic preconditioning; synaptic curvature; presynaptic mitochondria

ABSTRACT Hypoxic preconditioning (HPC) elicits resistance to more drastic subsequent insults, which potentially provide neuroprotective therapeutic strategy, but the underlying mechanisms remain to be fully elucidated. Here, we examined the effects of HPC on synaptic ultrastructure in olfactory bulb of mice. Mice underwent up to five cycles of repeated HPC treatments, and hypoxic tolerance was assessed with a standard gasp reflex assay. As expected, HPC induced an increase in tolerance time. To assess synaptic responses, Western blots were used to quantify protein levels of representative markers for glia, neuron, and synapse, and transmission electron microscopy was used to examine synaptic ultrastructure and mitochondrial density. HPC did not significantly alter the protein levels of astroglial marker (GFAP), neuron-specific markers (GAP43, Tuj-1, and OMP), synaptic number markers (synaptophysin and SNAP25) or the percentage of excitatory synapses versus inhibitory synapses. However, HPC significantly affected synaptic curvature and the percentage of synapses with presynaptic mitochondria, which showed concomitant change pattern. These findings demonstrate that HPC is associated with changes in synaptic ultrastructure. **Synapse 69:7–14, 2015.**

INTRODUCTION

Ischemic/hypoxic preconditioning (I/HPC) is defined as a sublethal hypoxic exposure that elicits tissue or organ resistance to a subsequent and more drastic ischemic or hypoxic insults (Murry et al., 1986). Numerous studies have demonstrated the efficacy of HPC in multiple model systems, but the underlying mechanisms are not fully understood.

In the context of stroke, HPC has been shown to effectively protect neurons (Liu et al., 2000). Ischemic and hypoxic insults resulted in synaptic ultrastructural perturbations (Martone et al., 1999, Ito et al., 2006, Kovalenko et al., 2006). Considering that neuronal function and recovery after cerebral ischemia requires synaptic integrity (Murphy and Corbett, 2009), it is not surprising that modulation of synaptic responses plays a vital role in the pathophysiology of temporary and permanent cerebral ischemia. Is it possible that analogous alterations in synaptic ultrastructure and function may also contribute to the protective mechanisms of HPC? Olfactory bulb, part of brain, is rich of synapse and relevant to both HPC and stroke, which provides perfect target for current study. In this study, we used a model of repeated hypoxia-reoxygenation in mice to explore the

Contract grant sponsor: National Natural Science Foundation of China; Contract grant number: 81200915.

*Correspondence to: Xunming Ji, Xuanwu Hospital, Capital Medical University, 45 Changchun Street, Xicheng District, Beijing 100053, China. E-mail: jixm@ccmu.edu.cn

Y.L. and Z.S. contributed equally to this work.

Received 6 May 2014; Revised 21 July 2014; Accepted 8 August 2014

DOI: 10.1002/syn.21777

Published online 25 August 2014 in Wiley Online Library (wileyonlinelibrary.com).

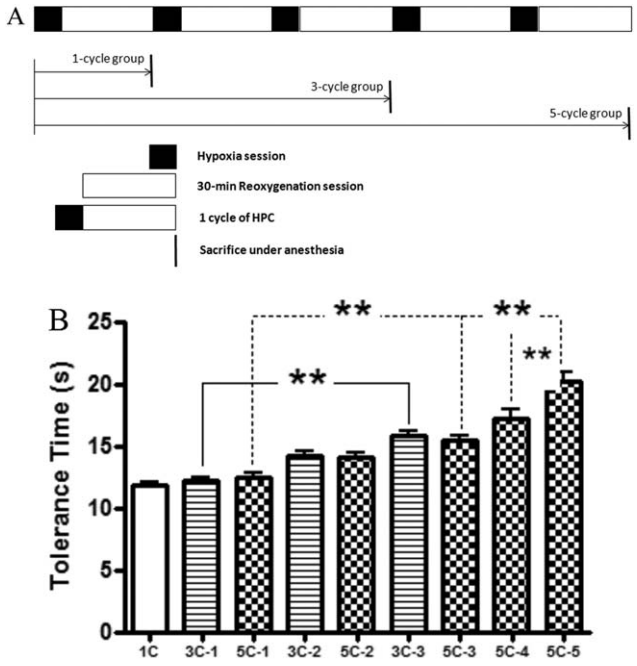

Fig. 1. HPC prolongs tolerance time. **A**: Protocol used in this study. Filled and blank rectangular boxes refer to hypoxia session and 30-min reoxygenation session respectively, which together comprise of 1-cycle HPC. The mice were sacrificed at the end of the last reoxygenation session in each group. **B**: Hypoxic tolerance time gradually increased as HPC treatments increased. $N = 15–32$. 1C, 3C, and 5C in *X*-axis refer to 1-cycle, 3-cycle, and 5-cycle HPC treatment group, respectively. 3C-1 means the first cycle in the 3-cycle group, and 3C-2 means the second cycle in the 3-cycle group, etc. SEM, standard error of the mean. $^{**}P < 0.01$.

responses in synaptic markers and synaptic ultrastructure. Our findings suggest that independent of any detectable change in synaptic proteins, HPC induced significant changes in synaptic curvature, which is concomitant with mitochondria density variations.

EXPERIMENTAL PROCEDURES

Animals

Male ICR mice ranging from 21 to 26 g were obtained from Beijing Vital River Experimental Animal Co. (Beijing, China). Animals were separated into four groups, control, 1-cycle, 3-cycle, and 5-cycle HPC treatment groups. Each group contained 15–32 mice with 6 mice for Western blots and 3 mice for transmission electron microscopy (TEM) analyses. Animals were randomly group-housed in a standard animal care room with the temperature $22 \pm 1°C$, the humidity $50 \pm 5\%$, and 12-h light/dark cycle. Animals were acclimatized to the environment and provided with chow and water ad libitum.

Hypoxic preconditioning

All procedures in this study were conducted according to the guidelines set by the University Animal Care and Use Committee of Capital Medical University and were consistent with the NIH Guide for the care and use of laboratory animals (NIH Publications No. 80-23). HPC mouse model was prepared as described with minor modifications (Zhang et al., 2011, Liu et al., 2012). End of each HPC was defined when the mouse presented gasp reflex. The 125-ml Jar was replaced with a 125 ml bottle with a screw cap, which guaranteed air isolation.

Homogenization and Western blot

Olfactory bulbs (OBs) were homogenized in RIPA lysis buffer and certain amounts of protein with loading buffer were boiled at 100°C for 5 min and subjected to 12% Sodium dodecyl sulfate-polyacrylamide gel electropheresis (SDS-PAGE) (Liu et al., 2010). The antibodies dilutions were 1:500 for GAP-43 and GFAP (Santa Cruz, CA, USA), 1:2000 for synaptophysin (MBL, Nagoya, Japan), 1:4000 for SNAP25 (BD Biosciences, San Jose, CA, USA), OMP (WAKO, Richmond, VA, USA), and Tuj-1 (Abcam, Cambridge, UK) and 1:3000 for GAPDH (Sigma-Aldrich, Missouri, USA).

Electron microscopy

TEM was performed as described previously (Xian et al., 2009). Anesthetized mice were perfused transcardially with physiological saline followed by 2% paraformaldehyde and 2% glutaraldehyde in 0.1 M phosphate buffer (pH 7.4). Brains were removed and placed in 2.5% glutaraldehyde in the same buffer overnight. OBs were dissected transversely at 1 mm thickness, rinsed in 0.1 M PB, and post-fixed in 1% osmium tetroxide for 2 h. After rinsing in 0.1 M PB, samples went through dehydration in degraded acetone solutions and embedded in Epon resin. Toluidine blue stained semithin (500 nm) sections were used to localize neuron rich area. Ultrathin sections (70 nm) were stained with uranyl acetate and lead citrate. Pictures were recorded by TEM (FEI, TECNAI G220) with Gatan 894 CCD and analyzed with Gatan digital micrograph. The picture taken at a magnification of ×9900 was for synaptic density quantification; and magnification of ×26,500 was set for synaptic ultrastructural observation.

Synapse and mitochondria analyses

For synaptic density, both Gray type I (excitatory) and Gray type II (inhibitory) synapses were included. About 15–33 pictures were taken for each group.

For synaptic ultrastructure and mitochondrial density recording, only Gray Type I synapse was analyzed. About 112–154 pictures were analyzed for each group. Synaptic ultrastructure included synaptic perforation and synaptic curvature according to Petit's description (Weeks et al., 2003). Convex means postsynaptic bouton protruded into presynaptic terminal, whereas protrusion of presynaptic terminal into postsynaptic bouton is referred to as concave. All synapses were analyzed by professional technician blind to sample information.

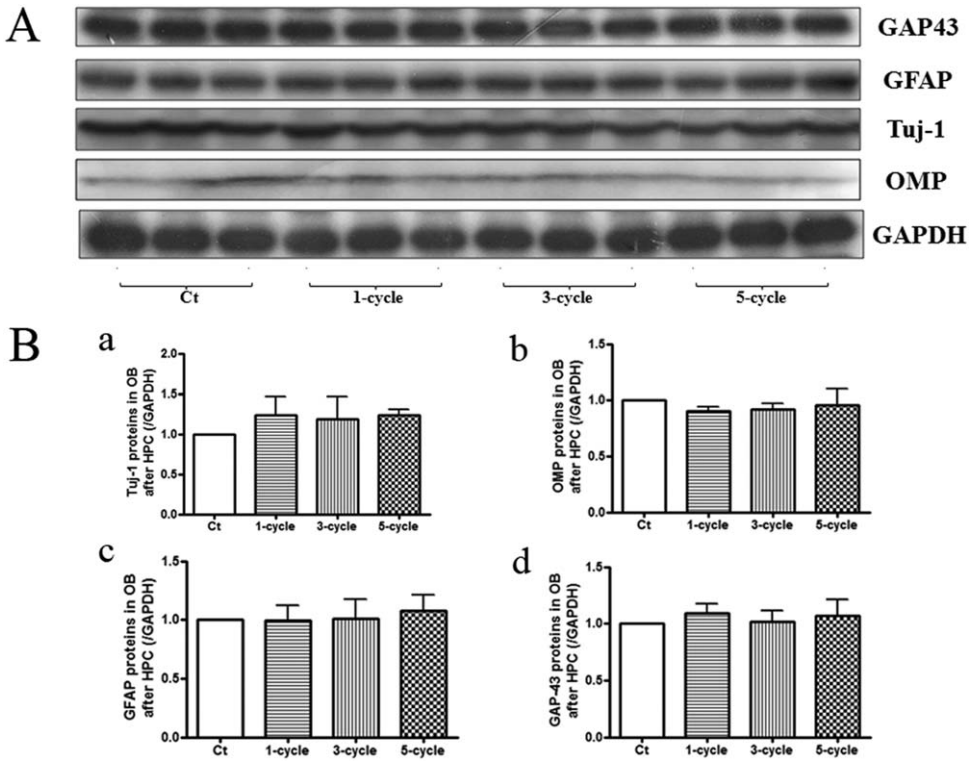

Fig. 2. Representative neuronal and astroglial markers are not affected by HPC. Western blots assay detected neuronal marker GAP43, olfactory neuronal maturation markers Tuj-1 and OMP, and astroglial marker GFAP (**A**). Statistical analyses did not show any significant changes between control and HPC treated groups (**B**). $N = 6$, SEM, standard error of the mean.

Data analysis

All data were expressed as group mean ± standard error of the mean (SEM). Data from tolerance time, Western blots assay, and synaptic ultrastructure analyses were subjected to a non-parametric ANOVA followed by Tukey: compare all pairs of columns. Statistical difference was set at $P < 0.05$.

RESULTS

HPC was performed by subjecting mice to repeated cycles of hypoxia and reoxygenation (Fig. 1A). A standard gasp reflex assay demonstrated as HPC treatments increased, tolerance time increased significantly, which were shown in comparison between the first cycle in 3-cycle group (3C-1) and the third cycle in 3-cycle group (3C-3), and between 5C-1 and 5C-3. Especially when HPC treatments increased more, tolerance time increased even faster, which were shown in comparison between 5C-3 and 5C-5, and between 5C-4 and 5C-5 (Fig. 1B).

Western blots showed that HPC did not alter the protein levels of representative markers for glia (GFAP), neuron (GAP43), and olfactory neuron maturation (Tuj1 and OMP) (Fig. 2). Further studies focused on synaptic ultrastructure. There were no significant differences in synaptic density between control and HPC groups detected by TEM (Figs. 3A and 3B) and by Western blots assay of synaptic number markers, synaptophysin, and SNAP25 (Fig. 3C). HPC did not affect the percentages of Gray type I (excitatory) synapse and Gray type II (inhibitory) synapse, the percentage of synaptic perforations, or average perforation per synapse significantly (Fig. 4). However, further analyses of synaptic curvature revealed significant changes by repeated HPC treatment. 3-cycle HPC treatment significantly decreased the percentage of flat synapses, while increased the percentage of convex synapses and sum of convex and concave synapses (Fig. 5). Concomitantly, the percentage of synapse with presynaptic mitochondria was significantly elevated by 3-cycle HPC treatment (Fig. 6A). Interestingly, both synaptic curvature and mitochondria distribution changes returned to normal level after 5-cycle HPC treatment. A similar pattern was observed for average presynaptic mitochondria number per synapse, but lack of statistical significance (Fig. 6C). Neither percentage of synapse with postsynaptic mitochondria nor average

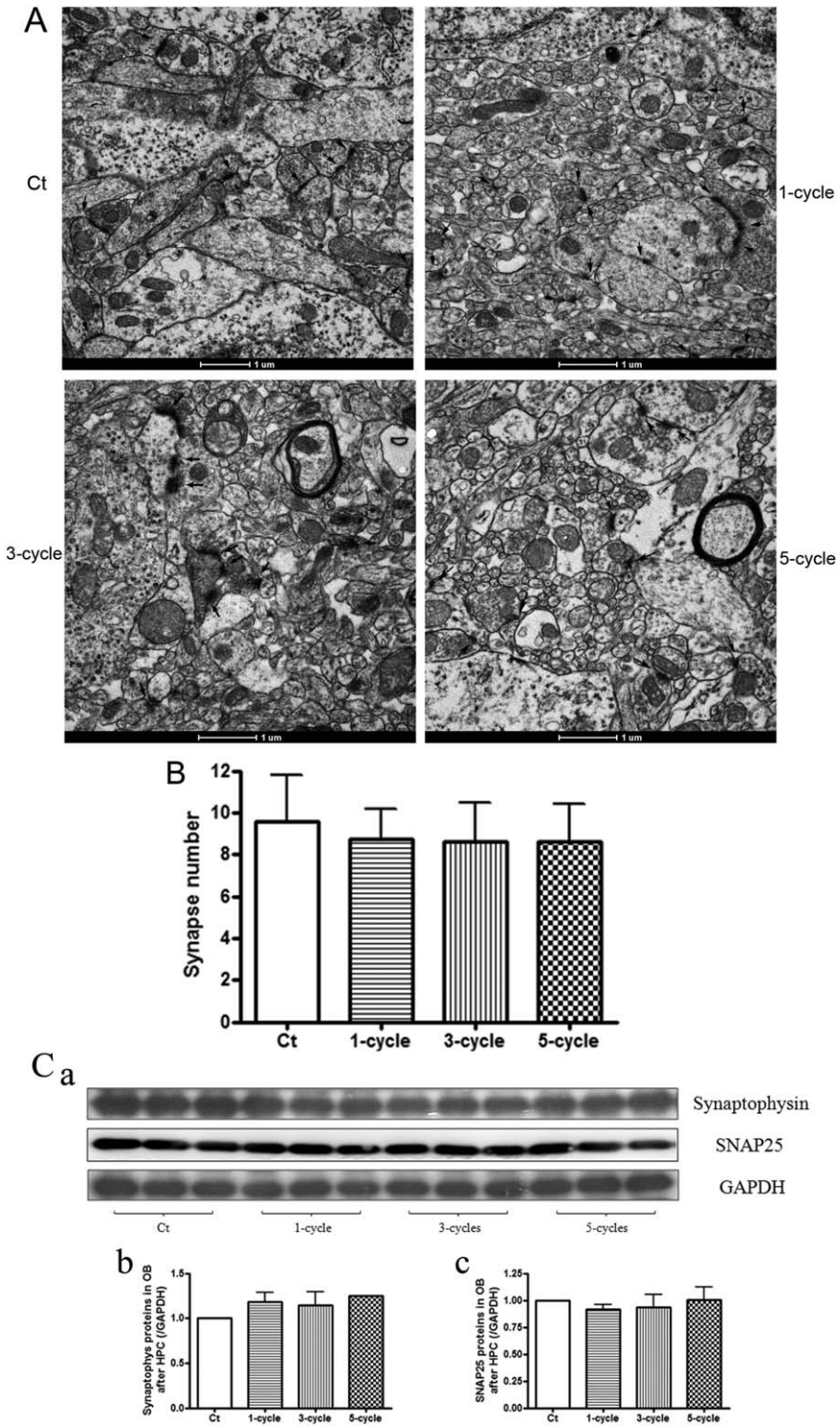

Fig. 3. Synaptic number is not affected by HPC. Synapse was illustrated with arrows in (**A**). Synaptic number was evaluated by TEM quantification with low magnification (A, **B**) and Western blots assay of synaptic number marker synaptophysin and SNAP25 (**C**). Both statistical analyses showed consistently that synaptic number was not affected by HPC. For TEM, 5–11 pictures were used for each mouse, $N = 3$. For Western blot, $N = 6$. SEM, standard error of the mean.

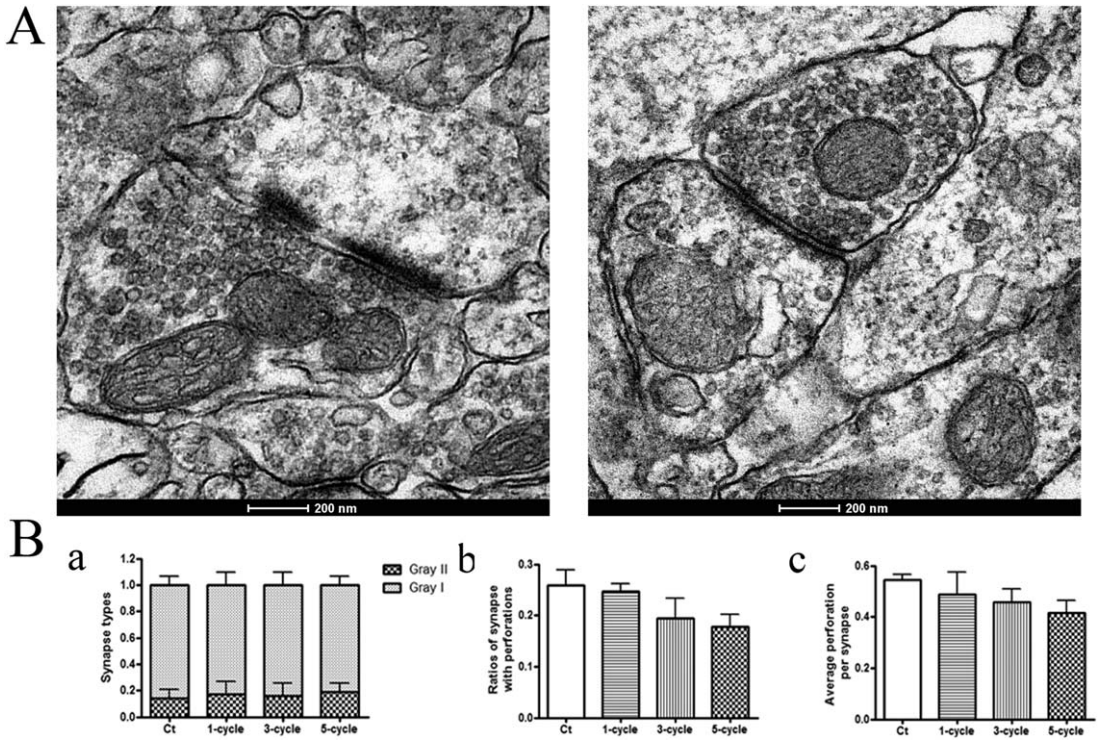

Fig. 4. Synaptic type and perforation are not affected by HPC. Both Gray type I (left) and Gray type II (right) synapses were recorded and shown (**A**), and their percentages were calculated (**B**), which didn't present significant changes. Ratios of perforated synapse and average perforation per synapse showed decrease tendency as HPC treatments increased; however, the statistical analysis results were negative (B). $N = 3$, SEM, standard error of the mean.

postsynaptic mitochondria number per synapse showed any significant changes (Figs. 6B and 6D).

DISCUSSION

In this study, synaptic ultrastructural changes in mice by repeated HPC treatments were elaborately studied. Results showed that repeated HPC significantly affected synaptic curvature and concomitantly affected presynaptic mitochondrial density. These findings suggest that the effects of HPC were mediated in part through synaptic ultrastructural changes.

HPC is part of a broad array of preconditioning and tolerance phenomena that is highly conserved throughout evolution. Various stimuli such as ischemia, hypoxia, hypothermia, and any conditions that cause stress may induce a preconditioned response (Gidday, 2006). Interestingly, repeated HPC elicites tissue/organ resistance to subsequent more drastic ischemic/hypoxic insults, which can be divided into rapid and delayed tolerance, with protections developing from minutes to days (Shpargel et al., 2008). The mechanisms included immediate release of mediators, rapid post-translational modifications of preexisting proteins (Tsai et al., 2004), and activation of signal transduction pathway for de novo synthesization of protective proteins (Kamota et al., 2009). However, synaptic response to preconditioning are rarely examined.

Instead of 3D-electron microscopy focusing on sophisticated ultrastructure of single synapse, we used conventional TEM to obtain ultrastructural information of many synapses. 5-cycle HPC took only 270 min, which was far less than the synaptic turnover time of 3 days. Synaptic density is more stable during synaptic electrical activity, such as LTP (long-term potentiation) and LTD (long-term depression), which occurred within a short period. And it has been considered that the central nervous system typically utilized changes in synaptic ultrastructure other than synaptic number as primary means to modulate synaptic efficacy (Connor et al., 2006; Marrone and Petit, 2002). Similarly, we found significant changes in synaptic curvature instead of synaptic number by HPC treatment.

How changes in synaptic ultrastructure affect synaptic function is an area of ongoing study. Increased synapses with convex or concave shape were confirmed to be related with elevations in synaptic activity (Connor et al., 2006, Medvedev et al., 2010; Marrone et al., 2005). Furthermore, alterations in synaptic curvature could occur as quickly as 30 min

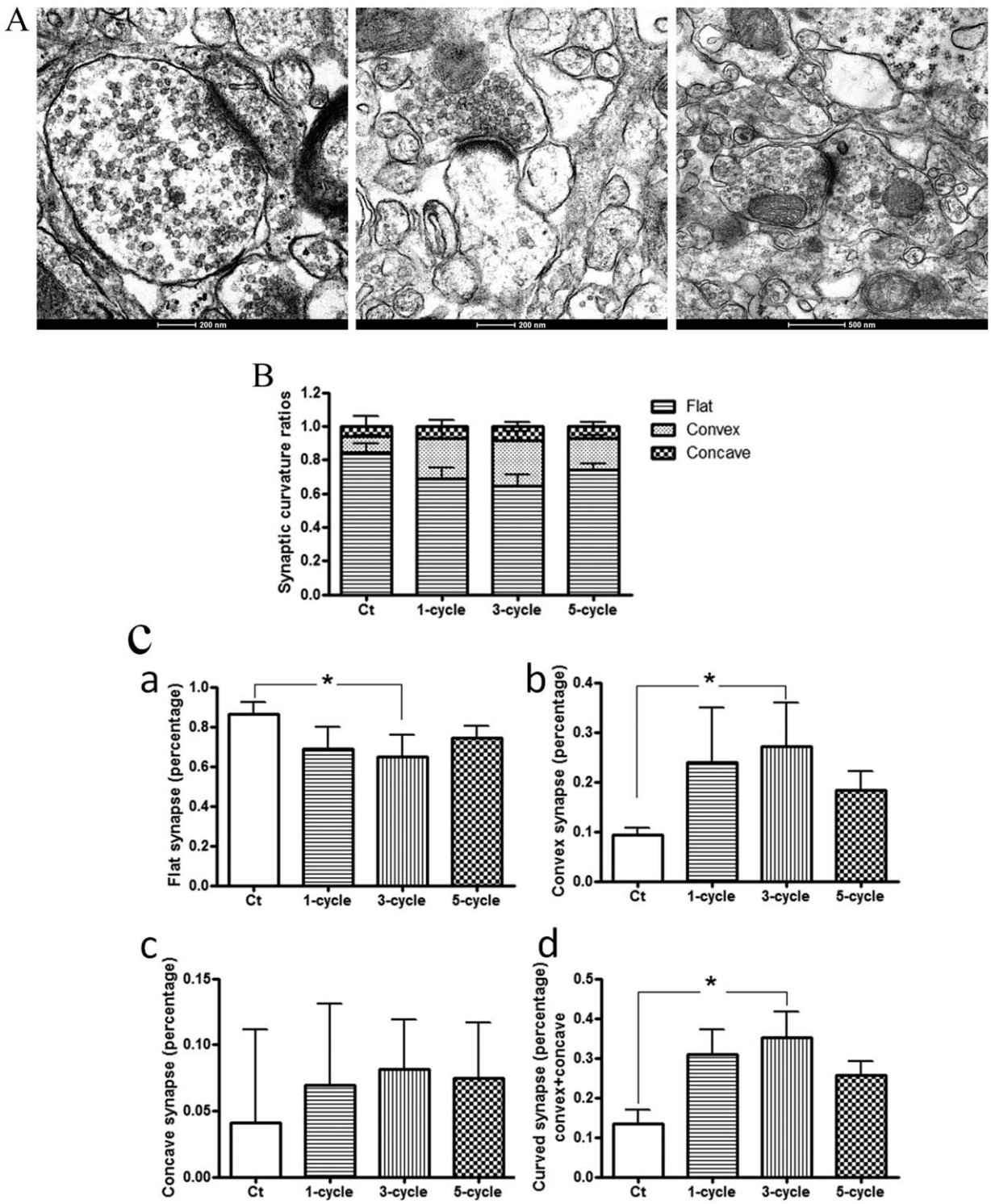

Fig. 5. HPC changes synaptic curvature. Typical synaptic curvatures: flat, convex, and concave were shown from left to right respectively (**A**), and their percentages were calculated (**B**). Further statistical analyses (**C**) identified significant decrease of percentage of flat synapse in 3-cycle HPC group compared with control group, whereas percentage of convex and sum of convex and concave synapses increased significantly. However, 5-cycle HPC treatment returned these changes to normal level. $N = 3$, SEM, standard error of the mean. $^*P < 0.05$.

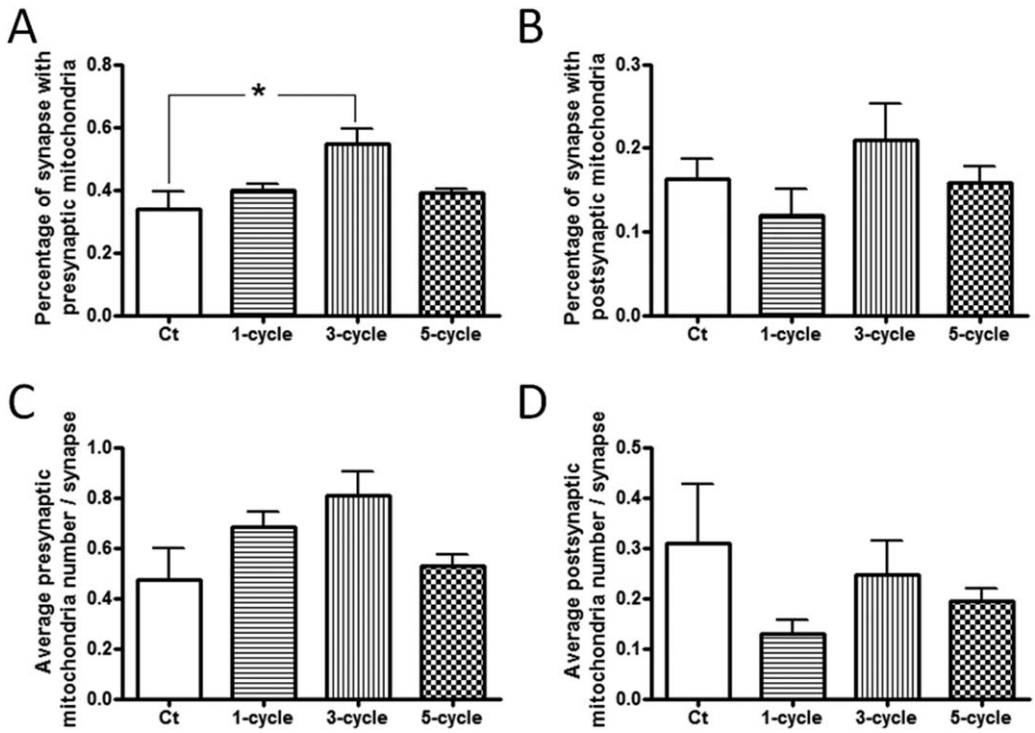

Fig. 6. HPC changes synaptic mitochondria distribution. Percentage of synapse with presynaptic mitochondria increased significantly by 3-cycle HPC and returned to normal level by 5-cycle HPC (**A**). Average presynaptic mitochondria number per synapse showed similar change pattern, however, the difference was not statistically significant (**C**). Neither percentage of synapse with postsynaptic mitochondria nor average postsynaptic mitochondria number per synapse showed significant difference (**B**, **D**). $N = 3$, SEM, standard error of the mean. $^*P < 0.05$.

(Markus and Petit, 1989), which provided theoretical support for the present study. In this study, 5-cycle HPC normalized synaptic curvature changes caused by 3-cycle HPC. If true, these rapid alterations in synaptic ultrastructure may require corresponding responses in energy utilization. Our results showed that, along with changes in synaptic curvature, the percentage of synapses with presynaptic mitochondria also changed. Thus, it is tempting to speculate that HPC triggers a coordinated set of energetic responses as part of endogenous homeostatic programs that allow synapses to adjust to subsequent insults. How these synaptic responses contribute to the beneficial induction of hypoxic tolerance and protective benefits of HPC warrants further investigation in future.

ACKNOWLEDGEMENT

The authors are grateful to Eng Lo for help with the editing of the manuscript. The authors declare no conflicts of interest of this paper.

REFERENCES

Connor S, Williams PT, Armstrong B, Petit TL, Ivanco TL, Weeks AC. 2006. Long-term potentiation is associated with changes in synaptic ultrastructure in the rat neocortex. Synapse 59:378–382.

Gidday JM. 2006. Cerebral preconditioning and ischaemic tolerance. Nat Rev Neurosci 7:437–448.

Ito U, Kuroiwa T, Nagasao J, Kawakami E, Oyanagi K. 2006. Temporal profiles of axon terminals, synapses and spines in the ischemic penumbra of the cerebral cortex: Ultrastructure of neuronal remodeling. Stroke 37:2134–2139.

Kamota T, Li TS, Morikage N, Murakami M, Ohshima M, Kubo M, Kobayashi T, Mikamo A, Ikeda Y, Matsuzaki M, Hamano K. 2009. Ischemic pre-conditioning enhances the mobilization and recruitment of bone marrow stem cells to protect against ischemia/reperfusion injury in the late phase. J Am Coll Cardiol 53: 1814–1822.

Kovalenko T, Osadchenko I, Nikonenko A, Lushnikova I, Voronin K, Nikonenko I, Muller D, Skibo G. 2006. Ischemia-induced modifications in hippocampal CA1 stratum radiatum excitatory synapses. Hippocampus 16:814–825.

Liu J, Ginis I, Spatz M, Hallenbeck JM. 2000. Hypoxic preconditioning protects cultured neurons against hypoxic stress via TNF-alpha and ceramide. Am J Physiol Cell Physiol 278:C144–C153.

Liu Y, Ye Z, Yang H, Zhou L, Fan D, He S, Chui D. 2010. Disturbances of soluble N-ethylmaleimide-sensitive factor attachment proteins in hippocampal synaptosomes contribute to cognitive impairment after repetitive formaldehyde inhalation in male rats. Neuroscience 169:1248–1254.

Liu C, Peng Z, Zhang N, Yu L, Han S, Li D, Li J. 2012. Identification of differentially expressed microRNAs and their PKC-isoform specific gene network prediction during hypoxic pre-conditioning and focal cerebral ischemia of mice. J Neurochem 120:830–841.

Markus EJ, Petit TL. 1989. Synaptic structural plasticity: Role of synaptic shape. Synapse 3:1–11.

Marrone DF, Petit TL. 2002. The role of synaptic morphology in neural plasticity: Structural interactions underlying synaptic power. Brain Res Brain Res Rev 38:291–308.

Marrone DF, LeBoutillier JC, Petit TL. 2005. Ultrastructural correlates of vesicular docking in the rat dentate gyrus. Neurosci Lett 378:92–97.

Martone ME, Jones YZ, Young SJ, Ellisman MH, Zivin JA, Hu BR. 1999. Modification of postsynaptic densities after transient

cerebral ischemia: A quantitative and three-dimensional ultrastructural study. J Neurosci 19:1988–1997.

Medvedev NI, Popov VI, Dallerac G, Davies HA, Laroche S, Kraev IV, Rodriguez Arellano JJ, Doyere V, Stewart MG. 2010. Alterations in synaptic curvature in the dentate gyrus following induction of long-term potentiation, long-term depression, and treatment with the *N*-methyl-D-aspartate receptor antagonist CPP. Neuroscience 171:390–397.

Murphy TH, Corbett D. 2009. Plasticity during stroke recovery: From synapse to behaviour. Nat Rev Neurosci 10:861–872.

Murry CE, Jennings RB, Reimer KA. 1986. Preconditioning with ischemia: A delay of lethal cell injury in ischemic myocardium. Circulation 74:1124–1136.

Shpargel KB, Jalabi W, Jin Y, Dadabayev A, Penn MS, Trapp BD. 2008. Preconditioning paradigms and pathways in the brain. Cleve Clin J Med 75 (Suppl 2):S77–S82.

Tsai BM, Wang M, March KL, Turrentine MW, Brown JW, Meldrum DR. 2004. Preconditioning: Evolution of basic mechanisms to potential therapeutic strategies. Shock 21:195–209.

Weeks AC, Ivanco TL, Leboutillier JC, Marrone DF, Racine RJ, Petit TL. 2003. Unique changes in synaptic morphology following tetanization under pharmacological blockade. Synapse 47:77–86.

Xian X, Liu T, Yu J, Wang Y, Miao Y, Zhang J, Yu Y, Ross C, Karasinska JM, Hayden MR, Liu G, Chui D. 2009. Presynaptic defects underlying impaired learning and memory function in lipoprotein lipase-deficient mice. J Neurosci 29:4681–4685.

Zhang N, Yin Y, Han S, Jiang J, Yang W, Bu X, Li J. 2011. Hypoxic preconditioning induced neuroprotection against cerebral ischemic injuries and its cPKCgamma-mediated molecular mechanism. Neurochem Int 58:684–692.